Main-Chain Cholesteric Liquid Crystalline Polyesters with Chiral Pendant Groups. 2. Cholesteric Copolyesters Containing Chiral and Achiral Substituted Hydroquinones

Koichi Fujishiro† and Robert W. Lenz*

Polymer Science and Engineering Department, University of Massachusetts, Amherst, Massachusetts 01003

Received February 22, 1991; Revised Manuscript Received July 2, 1991

ABSTRACT: A series of copolyesters based on 2-[(*S*)-(+)-methyl-1-butoxy]hydroquinone as the chiral monomer with several nonchiral hydroquinones was synthesized to form a new family of main-chain cholesteric liquid crystalline polymers (ChLCPs) containing a flexible spacer. Copolymerization was effective in forming an identifiable cholesteric phase with a wide mesophase temperature range, which was influenced to some extent by the spacer length because the copolymers with a tetramethylene spacer unit did not show a typical cholesteric texture above the melting transition, but those with longer spacers did. The data obtained suggest that formation of the cholesteric phase in these polymers was influenced by a balance between the helical twisting power of the chiral substituent and the mobility of the main chains.

Introduction

The wide variety of thermotropic cholesteric liquid crystalline polymers (ChLCPs), which have been prepared for a variety of applications,[1] can be classified according to their molecular structures as principally either main-chain ChLCPs or side-chain ChLCPs,[2] although some combined types of main- and side-chain polymers have also been prepared.[3] In addition, mixtures of achiral nematic LCPs with optically active low molar mass liquid crystals have been studied extensively.[4] Of these various types, the main-chain ChLCPs, in which the backbone contains the mesogenic units, have been studied to a lesser extent than the others because their syntheses can be quite difficult.[5-8]

This report concerns the continuation of our study on a new family of main-chain cholesteric liquid crystalline polymers (ChLCPs) (II) which are based upon mesogenic units that have chiral pendant substituents. For the chiral mesogenic units, we chose a triad ester (II) obtained from 2-[(*S*)-(+)-2-methyl-1-butoxy]hydroquinone (I) and a monomer containing *p*-hydroxybenzoic acid residues with a connecting flexible spacers, as shown in Chart I.

The preparation and properties of homopolymers containing this unit (II, n = 6, 10) were described in our previous report.[9] Surprisingly, their temperature ranges for formation of liquid crystalline phases were very narrow, and the texture of their liquid crystalline phases did not develop to those expected for a cholesteric phase. In this report, we compare those properties to the properties of copolyesters of series III (see Chart I), which contained the same chiral units along with units based on either unsubstituted or achiral substituted hydroquinones.

Experimental Section

All monomers, including 2-[(*S*)-(+)-methyl-1-butoxy]hydroquinone (I), were prepared as previously described.[9] The copolymers were prepared by the step-growth polymerization reaction of I and the nonchiral substituted hydroquinones with an appropriate 4,4′-dichloroformyl-α,ω-diphenoxyalkane monomer in solution as previously described.[10] In most cases, the reaction mixtures remained homogeneous throughout, but the polymers with shorter flexible spacers, n = 4 or 5 in III, precipitated during the reaction. All polymers prepared were characterized for molecular weight, specific rotation, thermal transitions, and crystalline and liquid crystalline morphologies as previously described.[9] The molar fractions of the chiral monomer, I, in the copolymers having different compositions (III-1,2,3 and IV-1,2,3) were checked by 400-MHz ^{1}H NMR spectroscopy based on the integrated value of the methyl protons of the 2-methyl-1-butoxy group at 0.7–0.9 ppm and the 3,3′-aryl protons at 8.14 ppm for solutions of the copolyesters in deuterated trifluoroacetic acid. The differences between the molar fraction observed in the NMR spectra and the molar fraction of the monomers supplied for the polymerization were less than 3%, so the latter was shown in tables as the compositions of the copolymers.

Table I
Yields and Properties of Copolymers of Series III (Y = H)

polymer	comp[a] x	comp[a] y	yield, %	$[\eta]$,[b] dL/g	mol wt $\bar{M}_n$	mol wt $\bar{M}_w$	$\bar{M}_w/\bar{M}_n$	opt rot,[c] deg (c 2.5, $CHCl_3$)
III-1	20	80	79	0.29	*d*			*f*
III-2	50	50	90	0.93	62 000	130 000	2.1	+1.9
III-3	80	20	93	1.55	*e*			*g*

[a] Monomer composition supplied for polymerization. [b] Inherent viscosity in *p*-chlorophenol at 45.3 °C. [c] Measured at 20 °C. [d] A precipitate formed during polymerization. [e] Gelation occurred during polymerization. [f] The polymer was insoluble. [g] Gelation occurred in chloroform and true solution could not be obtained.

Results and Discussion

Copolymers Prepared from Hydroquinone (III, Y = H). The data for the preparation and properties of copolymers containing different contents of units based on monomer I and on the unsubstituted hydroquinone monomer are collected in Table I. The copolymers with higher contents of I, III-2 and III-3, had high molecular weights presumably because they were more soluble in the reaction solvent than copolymer III-1, which was not soluble. The higher molecular weight copolymers, III-2 and III-3, were fibrillar in appearance in the solid state while copolymer III-1 was a powder. Only copolymer III-2 was sufficiently soluble for measurement of optical activity, but it showed only a low specific rotation because of the relatively low content of the chiral monomer.

The thermal transitions for this series of copolymers as determined by differential scanning calorimetry (DSC) are listed in Table II and compared with those of the homopolymer, II-10, which was described in our previous

† Present address: Chemicals Research Laboratory, R&D Laboratories—1, Nippon Steel Corp., 1618 Ida, Nakahara-ku, Kawasaki 211, Japan.

0024-9297/92/2225-0088$03.00/0

Chart I

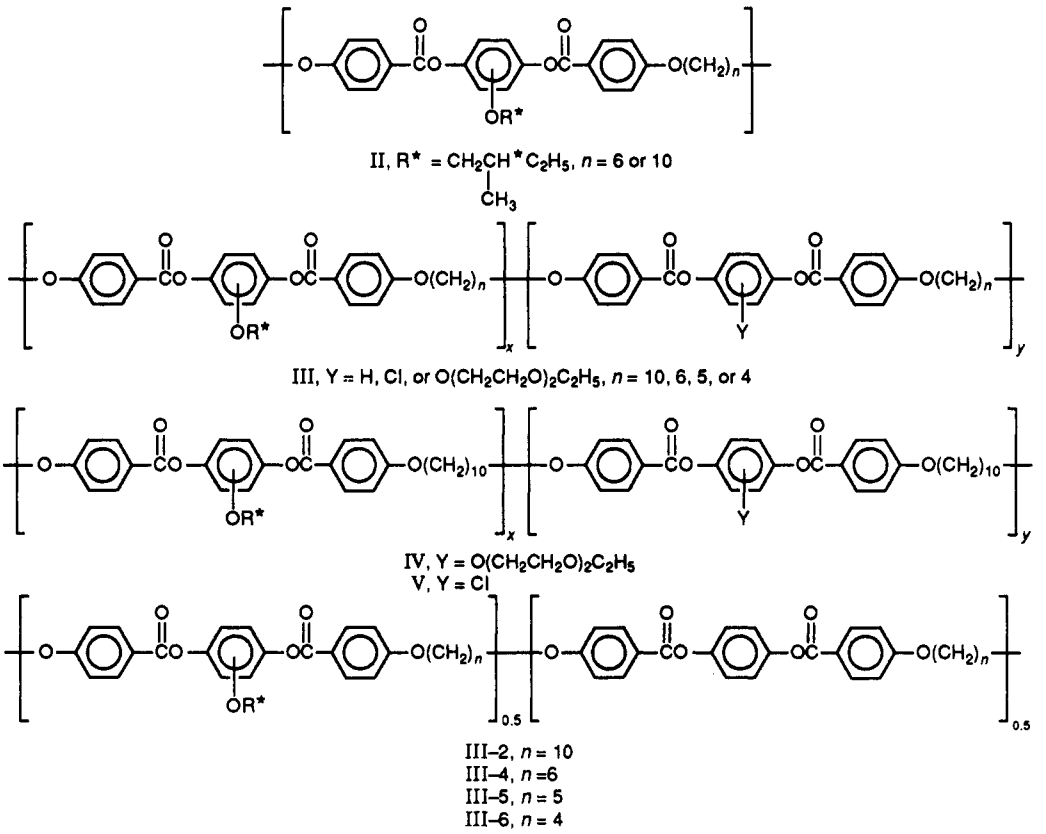

Table II
Transition Temperatures and Properties for Copolymers of Series III (Y = H)

	thermal transitions,[a] °C						thermodynamic properties[b]			
	heating cycle			cooling cycle						
polymer	T_m	T^*	T_i	T_c	T^*	T_d	ΔH_m, kcal/mru	ΔH^*, kcal/mru	ΔH_i, kcal/mru	ΔS_i, cal/(mru·K)
III-1	192	223	276	189	205	270	0.1	0.7	0.8	1.2
III-2	154	190	249	123	147	242	0.5	0.3	1.4	2.7
III-3	175		214	112		192	1.1		1.1	2.3
II-10[c]	148		158	112		151	1.6[d]		1.6[d]	3.2[d]

[a] Recorded from the second heating and cooling cycle at 20 °C/min scanning rate. T_m = crystalline to liquid crystalline transition; T^* = liquid crystalline to liquid crystalline transition; T_i = liquid crystalline to isotropic transition; T_c = recrystallization transition; T_d = isotropic to liquid crystalline transition. [b] Calculated from endotherms in second heating cycle and based on the repeating unit structure. [c] Polymer II (n = 10), from ref 9. [d] Calculated from exotherms in second cooling cycle and based on the repeating unit structure.

report.[9] The isotropization temperatures, T_i, of the copolymers were enhanced over that of the homopolymer so their mesophase temperature ranges were significantly wider as compared with those for polymer II-10 (n = 10).

The thermograms of copolymers III-1 and III-2 contained three endotherms in the heating cycle and three exotherms in the cooling cycle as seen in Figure 1 for copolymer III-2. Photomicrographs of this copolymer taken over a series of temperatures on a hot stage of a polarizing microscope are shown in Figure 2. The first endotherm in Figure 1 corresponded to the melting transitions, T_m, at which the sample became noticeably fluid. At the second endotherm, which is designated T^* in Table II, the melt viscosity of the samples sharply decreased. Above T_m, the copolymer exhibited a fine schlieren texture up to T^*, but this texture developed only very slowly during 3 days of annealing, presumably because of the relatively high melt viscosity of the sample. However, even after annealing above T^* for 2 days, it was still not possible to identify the type of the liquid crystalline phase present, as seen from the texture in Figure 2b. On cooling copolymer III-2 from the isotropic state, fine droplets appeared in the isotropic phase, as shown in Figure 2c, and these slowly coalesced into a typical planar cholesteric texture as shown in Figure 2d. On further cooling, the planar texture was converted into a chevron-like texture below 210 °C, as seen in Figure 2e.

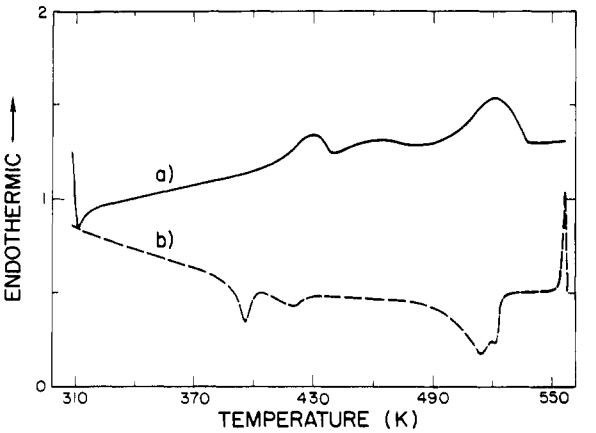

Figure 1. DSC thermograms of copolymer III-2 for (a) the second heating and (b) the second cooling cycle. (scanning rate, 20 °C/min).

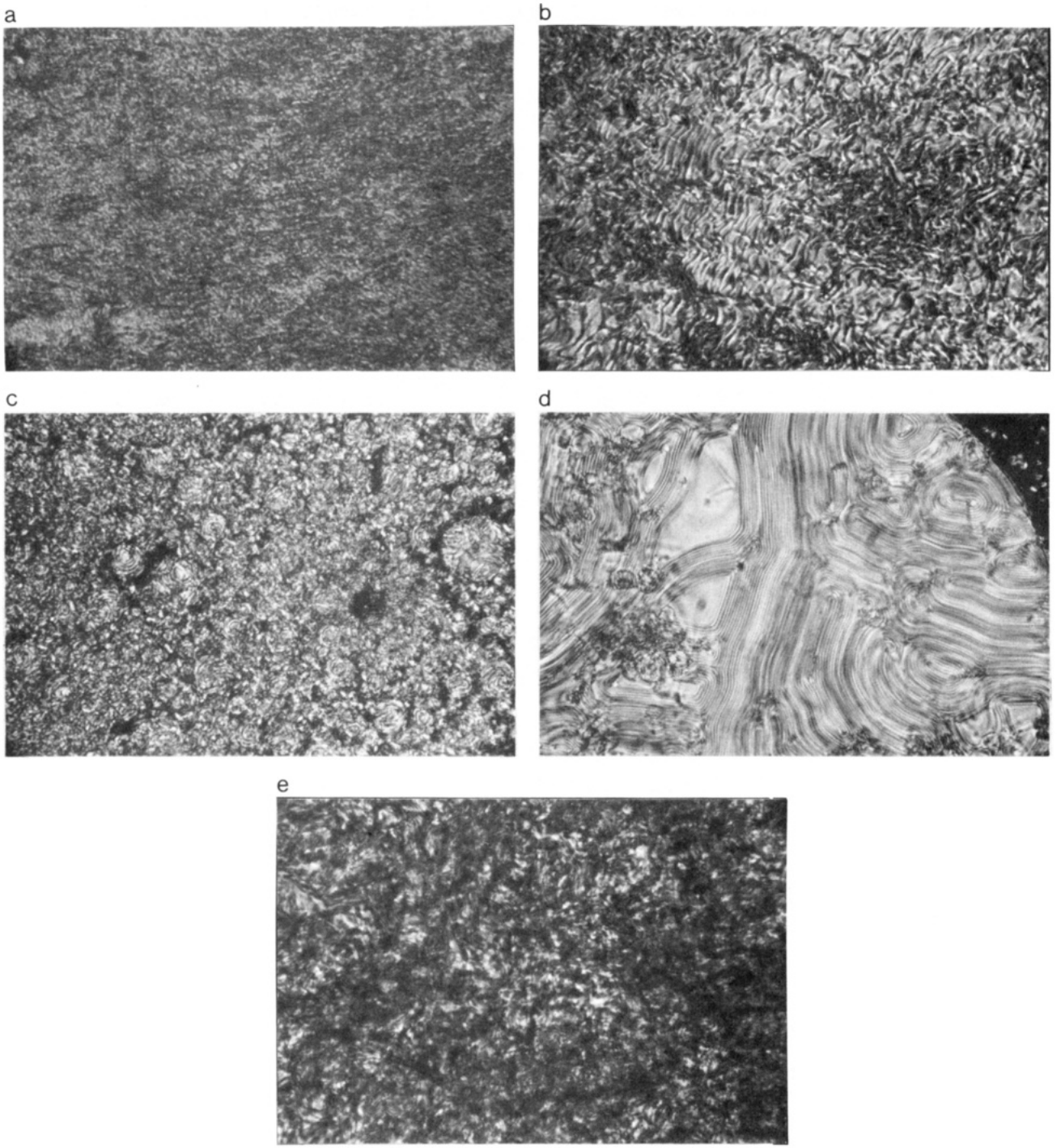

Figure 2. Photomicrographs of copolymer III-2: (a) 180 °C on heating; (b) 208 °C on heating; (c) 250 °C on cooling; (d) 226 °C on cooling; (e) 205 °C on cooling.

The thermograms for polymer III-1 also contained three endotherms in the second heating cycle. An oily streak texture was observed above T^* on heating, as shown in Figure 3a, and a planar texture (Figure 3b) and a chevron-like texture formed consecutively on cooling from the isotropic state. In contrast, the thermograms of polymer III-3 showed only two endotherms on heating, and a striated texture with regularly spaced retardation lines was observed in the heating and cooling cycles, as shown in Figure 3c.

Although these copolymers demonstrated different textures, all of the textures observed between T^* and T_i were characteristic of the cholesteric phase, and most likely both the amount of the chiral units in the copolymers and the molecular weights of the copolymers were important in the formation of the textures of the cholesteric phase. For example, the lower molecular weight copolymer, polymer III-1 ($[\eta] = 0.29$ dL/g), showed clearly the expected oily streak texture (Figure 3a), while the higher molecular weight copolymer, polymer III-2 ($[\eta] = 0.93$ dL/g), did not exhibit a well-developed oily streak texture on heating (Figure 2b), even though both copolymers exhibited planar textures on cooling (Figures 2d and 3b). The molecular weight effect will be discussed in more detail.

WAXD Analysis. As discussed above, copolymerization resulted in a wider temperature range of the liquid crystalline phase, and characterization of polymers III-1, III-2, and III-3 by DSC and polarizing microscope techniques revealed that this series of copolymers formed two types of liquid crystal phases above T_m, one of which

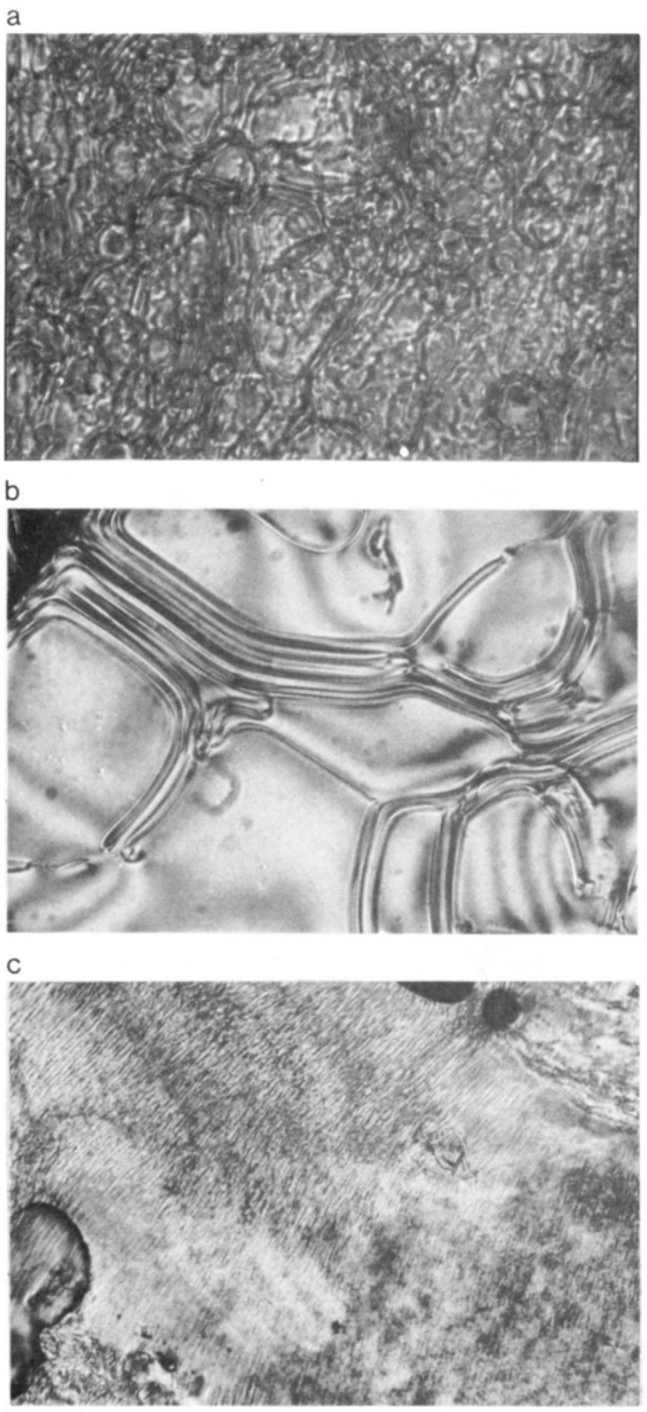

Figure 3. Photomicrographs of copolymers III-1 and III-3: (a) III-1 at 245 °C on heating; (b) III-1 at 270 °C on cooling; (c) III-3 at 200 °C on cooling.

showed the specific textures expected for a cholesteric phase between T^* and T_i, but the other phase between T_m and T^* could not be identified by the texture. Therefore, to obtain additional information on these phases, polymer III-2 was analyzed by wide-angle X-ray diffraction (WAXD). For this purpose, a sample of polymer III-2 was cooled from the isotropic state to room temperature and annealed at the X-ray measured temperature for 6 h in vacuo, after which the diffraction patterns were obtained. The results are collected in Figure 4 and Table III.

The diffraction pattern of polymer III-2 contained two outer rings at 4.40 and 4.28 Å (weak) and two inner rings at 17.9 and at 12.5–16.0 Å (diffuse) at 80 °C, as shown in Figure 4a. One of the inner rings at 12.6–17.7 Å became

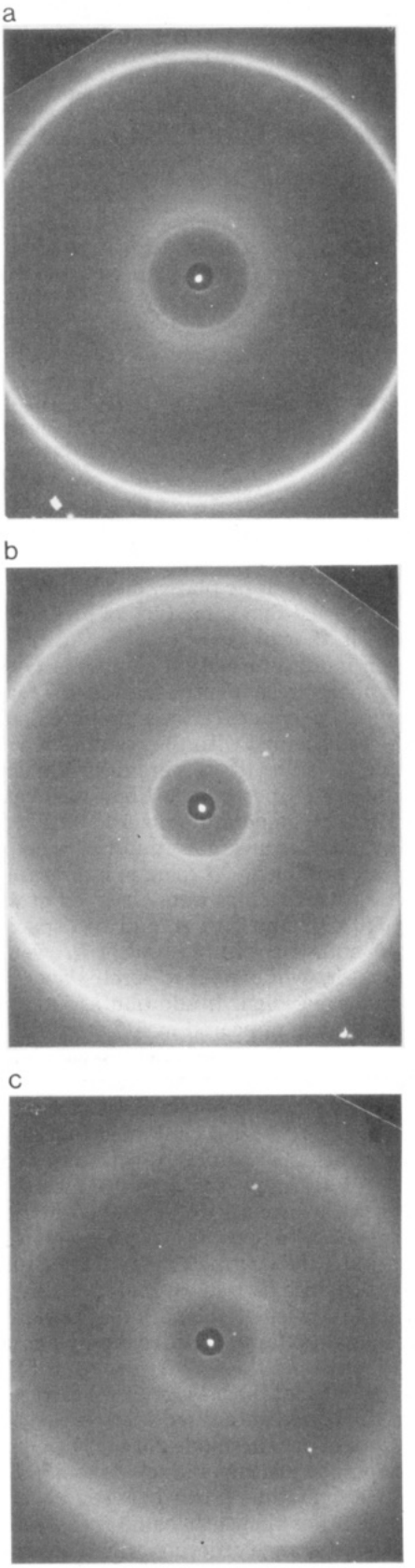

Figure 4. WAXD patterns of unoriented samples of copolymer III-2: (a) at 80 °C; (b) at 180 °C; (c) at 228 °C.

diffuse at 180 °C, but the other ring at 18.2 Å and the outer rings at 4.46 and 4.33 Å, which were accompanied by a diffuse halo at 4.1–5.3 Å, remained sharp at this temperature between T_m and T^*, as seen in Figure 4b. Above T^*, this polymer showed two diffuse rings at 4.3–5.3 and 14–21 Å, as seen in Figure 4c. The last pattern is consistent

Table III
Spacings for Unoriented and Oriented Samples of Polymer III-2

unoriented sample		oriented sample	
temp, °C	spacing, Å	temp, °C	spacing, Å
80	17.9	25	17.7; 51° from meridian
	12.5–16.0 (diffuse)		15.6; equator (diffuse)
			11.7; equator
	4.40		4.42; equator
	4.28		4.24; equator
			14.9; meridian
			9.77; meridian
			7.47; meridian
			5.97; meridian
			4.92; meridian
180	18.2	180	17.9; 51° from meridian
	12.6–17.7 (diffuse)		15.4; equator
			11.2; equator
	4.46		4.47; equator
	4.33		4.35; equator
	4.1–5.3 (diffuse)		
228	14–21 (diffuse)		
	4.3–5.3 (diffuse)		

with that of a cholesteric phase, but the two sharp rings in Figure 4b reveal that some type of higher order phase was present in that phase.

To obtain more information about the type of liquid crystalline phase present between T_m and T^*, an oriented fiber sample of polymer III-2 was prepared, and WAXD patterns were obtained with the results shown in Figure 5 and Table III. The fibers were drawn at 190–195 °C, which was above T^*, because the fibers were easily broken during drawing at temperatures below T^*. The fibers were annealed at 180 °C in an argon atmosphere before WAXD patterns were obtained. At room temperature, as shown in Figure 5a, two spacings were observed at wide angles equivalent to 4.42 and 4.24 Å, and two spacings at the small angles equivalent to 15.6 and 11.7 Å were observed on the equator, while weak discrete layer lines were observed on the meridian. In addition, a four-point pattern at a 17.7-Å spacing appeared at 51° from the meridian. These fibers were then placed in a glass capillary tube and heated at 180 °C in an X-ray apparatus with a hot stage, and WAXD patterns were obtained with the results shown in Figure 5b. The patterns contained four split spots at 51° from the meridian or 17.9 Å, with outer spacings on the equator at 4.47 and 4.35 Å (weak), which were still sharp, but no clear spacings were obtained on the meridian.

From the discrete spacings on the meridian for the crystalline state, the length of the repeating unit parallel to the main-chain axis was estimated as 29.7 Å, which corresponds to a calculated length for the repeating unit of 29.4 Å assuming a fully extended methylene chain. Two sharp outer rings and the 17.7-Å spacing at 51° from the meridian suggest that the mesogenic units were packed in layers, but the layers were tilted with respect to the fiber axis. This type of packing model for such a polymer crystal was also proposed by Atkins and co-workers.[11] In contrast, for the liquid crystalline phase between T_m and T^*, the packing pattern was almost the same as that below T_m but it lacked the long-range ordering, which possibly implies the presence of a cybotactic liquid crystalline phase. According to the cybotactic model proposed by Blumstein and co-workers,[5] the mesogenic units are still packed in tilted layers, but the layers are not arranged with long-range order relative to each other.

Compared with the homopolymer, polymer II-10, which had layers in the direction perpendicular to the fiber axis, as previously described,[9] copolymers with unsubstituted hydroquinone formed a tilted layer structure, presumably

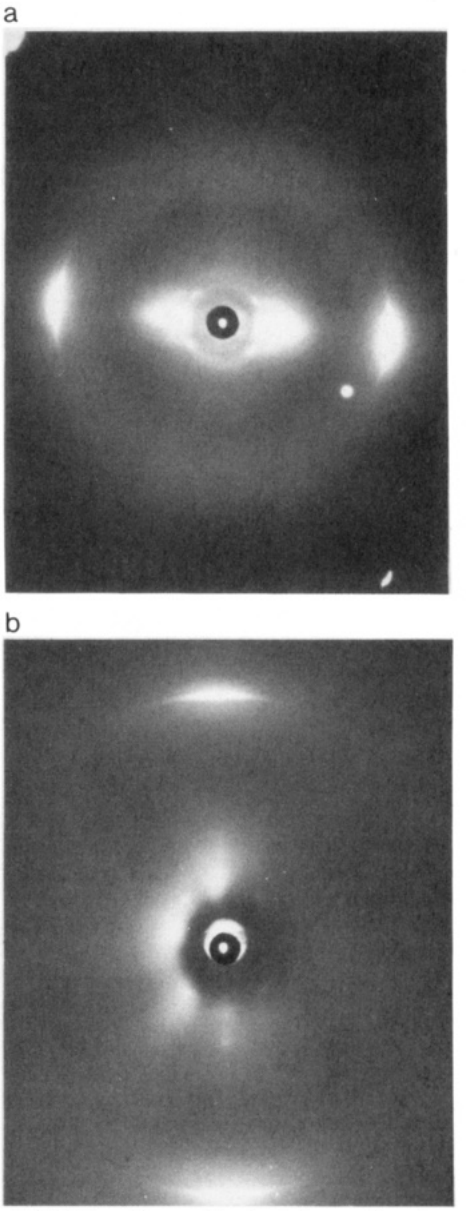

Figure 5. WAXD patterns of oriented samples of copolymer III-2: (a) annealed at 180 °C, measured at 25 °C; (b) annealed at 180 °C, measured at 180 °C.

because of the steric requirement for the packing of mesogenic units containing bulky pendant groups in the homopolymer.

Polymer III-1 gave the same WAXD patterns as polymer III-2 between transitions, but polymer III-3 showed only two diffuse rings between the T_m and T_i. Hence, it can be concluded that polymer III-1 had the same liquid crystalline phases as those proposed for polymer III-2, but polymer III-3 formed only a cholesteric phase above the melting transition.

Racemic Copolymers. A copolymer, III′, of the racemic monomer, 2-[(±)-2-methyl-1-butoxy]hydroquinone (I′), with hydroquinone was prepared and characterized for comparison with the chiral copolymer III-2, of the same composition. The racemic copolymer, III′, gave a very similar DSC thermogram to that of the chiral copolymer III-2, as shown in Figure 6, and the racemic copolymer exhibited a schlieren texture over the entire temperature range of the liquid crystalline states from T_m to T_i. However, the texture did not develop very well between T_m and T^*, and it was very similar in appearance to that of polymer III-2. Nevertheless, a well-developed schlieren

Table IV
Yields and Properties of Copolymers of Series IV and V

polymer	comp[a] x	comp[a] y	yield, %	[η], dL/g	mol wt $\bar{M}_n$	mol wt $\bar{M}_w$	$\bar{M}_w/\bar{M}_n$	opt rot,[b] deg (c 2.5, $CHCl_3$)
IV-1	20	80	98	0.91	72 000	202 000	2.8	+1.3
IV-2	50	50	85	1.01	47 000	160 000	3.4	+1.7
IV-3	80	20	75	0.42	14 000	48 000	3.4	+2.8
V	50	50	77	0.34	5 000	18 000	3.7	+2.0

[a] Monomer composition supplied for polymerization. [b] Measured at 20 °C.

Table V
Transition Properties for Copolymers of Series IV and V

polymer	thermal transitions, °C: heating cycle T_m	heating cycle T_i	cooling cycle T_c	cooling cycle T_d	thermodynamic properties[a] ΔH_m, kcal/mru	ΔH_i, kcal/mru	ΔS_i, cal/(mru·K)
IV-1	112	166	32, 90[b]	158	1.2	1.1	2.5
IV-2	123	165	78	154	1.2	1.3	3.0
IV-3	134	157	94	150	1.3	1.3	3.0
V	136	212	71, 104[b]	210	0.9	0.7	1.5

[a] Calculated from endotherms in the second heating cycle and based on the repeating unit structure. [b] Two endotherms were observed on cooling.

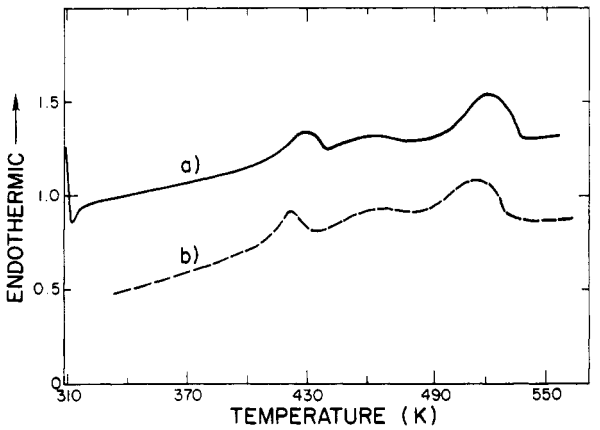

Figure 6. DSC thermograms of (a) chiral copolymer III-2 and (b) the racemic copolymer (Y = H, n = 10, $x = y = 0.5$; scanning rate, 20 °C/min).

texture could be formed by annealing between T^* and T_i. These observations confirmed that the chiral centers present in the pendant group can generate a cholesteric state but did not affect the transition temperatures of the copolymer, presumably because the degrees of ordering of the macromolecules in the mesogenic states are similar for the chiral and racemic copolymers, both of which apparently form nematic liquid crystalline states before isotropization.

Copolymers Prepared from Nonchiral Substituted Hydroquinones. Two series of copolymers of I with nonchiral substituted hydroquinones of the structures IV and V (Chart I) were prepared and characterized, and the results are collected in Tables IV and V and Figure 7:

The higher molecular weight copolymers, IV-1 and IV-2, were fiberlike in appearance in the solid state, while the others formed powders on precipitation. All of the polymers showed optical activity but with low specific rotations because of their decreased contents of I.

Most of the thermograms of the polymers showed two endotherms in the second heating cycle and two exotherms in the second cooling cycle except for polymers IV-1 and V, which exhibited three exotherms on cooling. The highest temperature transition for each polymer was taken as the isotropization temperature, as indicated by observations of samples on the hot stage of a polarizing microscope. Polymer IV-1 formed an oily streak texture during both its heating and cooling cycles, as shown in Figure 7a, while polymers IV-2 formed only a striated texture, as shown in Figure 7b. Polymer IV-3 did not show a clearly definable texture, but instead it formed fine domains having mainly two colors, as seen in Figure 7c. The colors changed from yellow-green to green to blue to purple to red to orange and finally back to yellow with a 180° rotation of the polarizer from the cross-polar position. Chiellini and co-workers also observed the same phenomenon for polymers with higher contents of chiral units, but the polymers did not show typical cholesteric textures.[6] Polymer V formed an oily streak texture in the heating cycle up to T_i, and on cooling from above T_i, it formed a planar texture, as shown in Figure 7d.

The WAXD patterns of unoriented samples of all of the polymers in series IV and polymer V gave two diffuse rings above T_m. Hence, it can be concluded that all of these copolymers formed clearly identifiable cholesteric phases instead of the unidentified phase formed by polymer III-2.

Effect of Spacer Length *n*. A series of copolymers of I and hydroquinone were prepared with monomers having different spacer lengths, n, as follows: III-2 (n = 10), III-4 (n = 6), III-5 (n = 5), and III-6 (n = 4), with the structures shown in Chart I.

The liquid crystalline properties of these copolymers are given in Table VI, and photomicrographs of their textures in the liquid crystalline state are shown in Figure 8. The copolymers with hexamethylene (III-4) and pentamethylene (III-5) spacers showed three transitions in their DSC thermograms, which, as before, were assigned to T_m, T^*, and T_i. The enthalpies of the transitions for T^* slightly decreased with decreasing spacer length, and the copolymer with the tetramethylene spacer (III-6) did not show the T^* transition.

Polarized light microscopy showed the presence of an oily streak texture during the heating cycle and a planar texture during the cooling cycle for polymers III-4 and III-5, as shown in Figure 8a,b, while polymer III-6 did not show a texture corresponding to that expected for a cholesteric phase, as seen in Figure 8c. Possibly the tetramethylene spacer formed a backbone that was rigid enough to restrict the organization into the helical structure of the cholesteric phase, and the high T_m of this polymer can be taken as an indication of increasing rigidity of the main chain. Strzelecki and Van Luyen also reported that, for

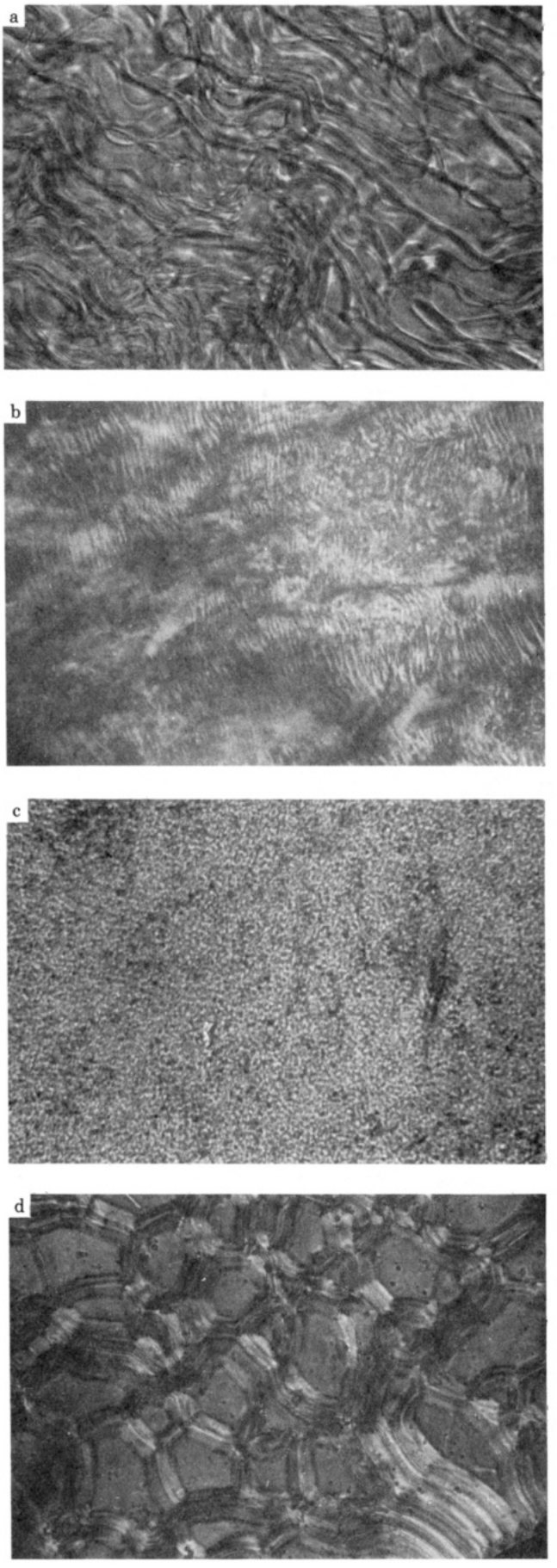

Figure 7. Photomicrographs of copolymers of series IV and copolymer V: (a) IV-1 at 160 °C on cooling; (b) IV-2 at 140 °C on cooling; (c) IV-3 at 147 °C on cooling; (d) V at 186 °C on cooling.

Table VI
Effects of Spacer Length (n) on Properties

polymer	n	thermal transitions,[a] °C T_m	T^*	T_i	$[\eta]$,[b] dL/g	texture
III-2	10	154	190	249	0.93	planar
III-4	6	184	228	290	0.25	oily streak, planar
III-5	5	172	230	285	0.34	oily streak, planar
III-6	4	207		320	0.21	schlieren

[a] Recorded from the second heating cycle. [b] Inherent viscosity in *p*-chlorophenol at 45.3 °C.

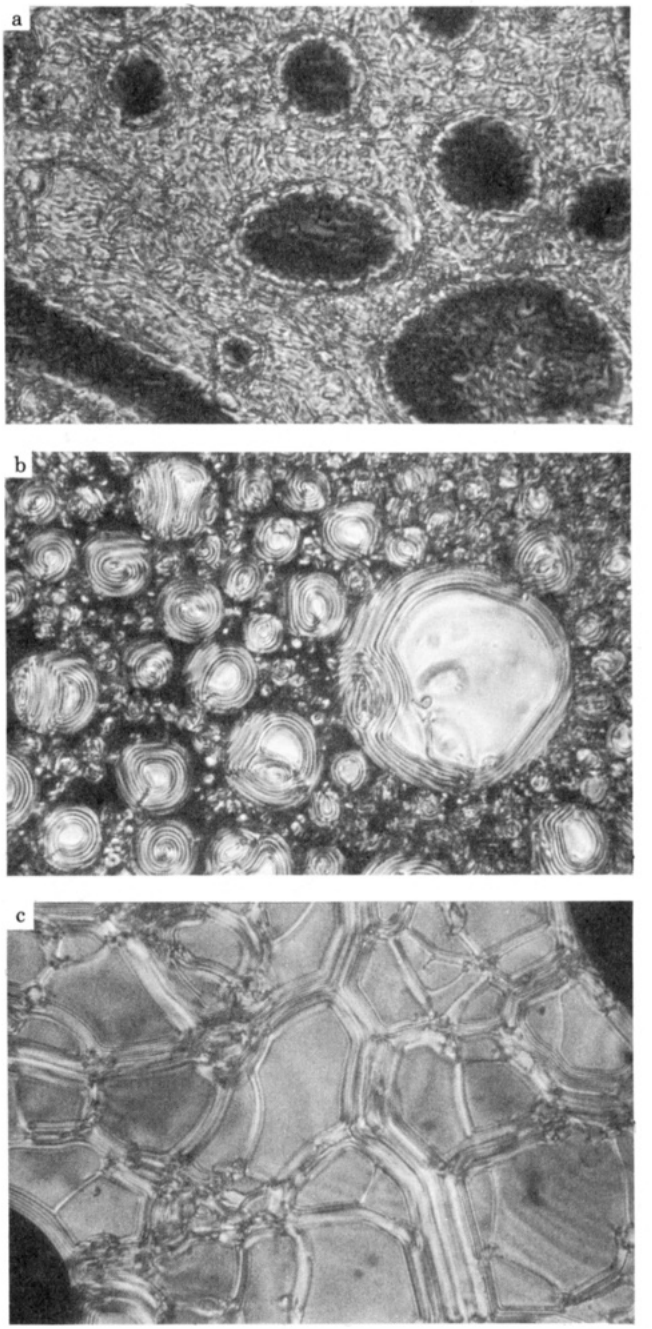

Figure 8. Photomicrographs of copolymers III-4, II-5, and III-6: (a) III-4 at 268 °C on cooling; (b) III-5 at 253 °C on cooling; (c) III-6 at 290 °C on cooling.

a series of LCPs with polymethylene flexible spacers, sharp decreases in transition temperatures were observed with spacer lengths above a value of $n = 4$.[12]

In summary, the data for the copolymers of series III, IV, and V, taken together, strongly support the proposal that formation of a cholesteric phase is influenced by a

balance between the helical twisting power of the chiral substituent and the mobility of the main chains in main-chain ChLCPs. In the systems studied in this investigation, the chiral mesogenic unit was always a triad ester unit containing 1,4-bis[(4-alkoxybenzoyl)oxy]-2-[(*S*)-2-methyl-1-butoxy]benzene groups, so the helical twisting power was constant, but the response of the polymers changed with the spacer length and presumably also with packing ability of the nonchiral mesogenic groups when the latter were present, so that both copolymerization with other hydroquinone derivatives having less bulky substituents and increasing the spacer length increased the mobility of the main chains and permitted the cholesteric phase to form.

Conclusion

Copolymers containing unsubstituted hydroquinone units formed two liquid crystalline phases, one of which was a cholesteric phase, but the other may have been a cybotactic nematic phase. Copolymers with nonchiral substituted hydroquinone units formed only a cholesteric phase.

Acknowledgment. We greatly appreciate the financial support of Nippon Steel Corp., which made this work possible, and we thank Professor H. G. Zachmann of the University of Hamburg and Professor Koji Tashiro of Osaka University for useful discussions on the interpretation of the WAXD results.

References and Notes

(1) McDonell, D. G. In *Thermotropic Liquid Crystals*; Gray, G. W., Ed.; John Wiley & Sons: New York, 1987; p 120.
(2) Chiellini, E.; Galli, G. In *Recent Advances in Liquid Crystalline Polymers*; Chapoy, L. L., Ed.; Elsevier Applied Science Publishers: London and New York, 1985; p 15.
(3) (a) Bualek, S.; Zentel, R. *Makromol. Chem.* **1988**, *189*, 797. (b) Kapitza, H.; Zentel, R. *Makromol. Chem.* **1988**, *189*, 1793.
(4) (a) Noël, C.; Friedrich, C.; Laupretre, F.; Billard, G.; Bosio, L.; Strazielle, C. *Polymer* **1984**, *25*, 263. (b) Noël, C.; Laupretre, F.; Friedrich, C.; Fayolle, B.; Bosio, L. *Polymer* **1984**, *25*, 809. (c) Noël, C.; Friedrich, C.; Bosio, L.; Strazielle, C. *Polymer* **1984**, *25*, 1281.
(5) Blumstein, A.; Vilasagar, S.; Ponrathnam, S.; Clough, S. B.; Blumstein, R. B. *J. Polym. Sci., Polym. Phys. Ed.* **1982**, *20*, 877.
(6) Chiellini, E.; Galli, G.; Carrozzino, S.; Gallot, B. *Macromolecules* **1990**, *23*, 2106.
(7) Park, H. J.; Jin, J.; Lenz, R. W. *Polymer* **1985**, *26*, 1301.
(8) (a) Malanga, C.; Spassky, N.; Menicagli, R.; Chiellini, E. *Polym. Bull.* **1983**, *9*, 328. (b) Chiellini, E.; Galli, G.; Malanga, C.; Spassky, N. *Polym. Bull.* **1983**, *9*, 336.
(9) Fujishiro, K.; Lenz, R. W. *Macromolecules*, preceding paper in this issue (part 1).
(10) Lenz, R. W.; Furukawa, A.; Bhowmik, P.; Garay, R.; Majnusz, J. *Polymer* **1991**, *32*, 1703.
(11) Atkins, E. D. T.; Thomas, E. L.; Lenz, R. W. *Mol. Cryst. Liq. Cryst.* **1988**, *155*, 271.
(12) Strzelecki, L.; van Luyen, D. *Eur. Polym. J.* **1980**, *16*, 299.

Registry No. III-2 ($n = 10$), 137175-24-7; III-4 ($n = 6$), 137175-25-8; III-5 ($n = 5$), 137175-26-9; III-6 ($n = 4$), 137175-27-0; IV, 137175-28-1; V, 137175-29-2.